Universität des Saarlandes

Fachrichtung 6.1 – Mathematik

Preprint Nr. 194

On the Application of Projection Methods for Computing Optical Flow Fields

Thomas Schuster and Joachim Weickert

Saarbrücken 2007

Fachrichtung 6.1 – Mathematik
Universität des Saarlandes

Preprint No. 194
submitted: May 19, 2007

On the Application of Projection Methods for Computing Optical Flow Fields

Thomas Schuster

Fakultät für Maschinenbau
Helmut–Schmidt–Universität
Holstenhofweg 85
22043 Hamburg
Germany
schuster@hsu-hh.de

Joachim Weickert

Fakultät für Mathematik und Informatik
Universität des Saarlandes
Geb. E1.1
66041 Saarbrücken
Germany
weickert@mia.uni-saarland.de

Edited by
FR 6.1 – Mathematik
Universität des Saarlandes
Postfach 15 11 50
66041 Saarbrücken
Germany

Fax: + 49 681 302 4443
e-Mail: preprint@math.uni-sb.de
WWW: http://www.math.uni-sb.de/

Abstract

Detecting optical flow means to find the apparent displacement field in a sequence of images. As starting point for many optical flow methods serves the so called optical flow constraint (OFC), that is the assumption that the gray value of a moving point does not change over time. Variational methods are amongst the most popular tools to compute the optical flow field. They compute the flow field as minimizer of an energy functional that consists of a data term to comply with the OFC and a smoothness term to obtain uniqueness of this underdetermined problem. In this article we replace the smoothness term by projecting the solution to a finite dimensional, affine subspace in the spatial variables which leads to a smoothing and gives a unique solution as well. We explain the mathematical details for the quadratic and nonquadratic minimization framework, and show how alternative model assumptions such as constancy of the brightness gradient can be incorporated. As basis functions we consider tensor products of B-splines. Under certain smoothness assumptions for the global minimizer in Sobolev scales, we prove optimal convergence rates in terms of the energy functional. Experiments are presented that demonstrate the feasibility of our approach.

Keywords: optical flow, optical flow constraint, variational methods, projection methods, tensor product B-spline

MSC2000 Classification: 65F22, 68T45

1 Introduction

In digital image analysis, motion detection in image sequences is an important problem for tasks ranging from robot navigation to video compression. A key concept for characterizing motion in an image sequence is the notion of optical flow, the apparent displacement field between corresponding structures in subsequent images. The existing literature about optical flow problems is enormous. Thus, we only give a short overview which by far is not complete and refer the reader to [28, 38, 41] for more detailed surveys. Horn and Schunck [20] were the first to present an approach for a solution of the optical flow problem by minimizing an energy functional. The formulation of this functional relies on two fundamental assumptions: the constancy of brightness over time and a smoothness assumption. These requirements have been modified in numerous ways [1, 2, 4, 14, 15, 22, 29, 30, 32, 36, 42], but are still the starting point for todays variational solvers. Also in 1981 Lucas and Kanade [24] presented another approach which computes the optical flow field by solving a local least squares problem. The idea to see optical flow problems in the framework of inverse problems is not far fetched. Yet in 1988 Bertero, Poggio, and Torre [7] published a very nice overview of ill-posed problems in image analysis. They formulated the computation of optical flow as inverse problem and presented an approach by minimizing a Tikhonov-Phillips functional. Since the development of new solvers for the optical flow determination was very rapid in recent years, criteria to evaluate and compare the different methods became of growing importance. We quote Barron, Fleet, and Beauchemin [6] and Galvin et al. [16] as standard references concerning the evaluation of a number of classical optical flow methods. More recently, a variational method by Brox et al. [10] and subsequent modifications [3, 11, 12, 33] have led to highly accurate results. In spite of their complexity, at the heart of such methods is still the minimization of an energy functional consisting of a data and a regularization term.

The popularity of variational methods for regularizing the ill-posed problem of optical flow estimation serves also as starting point for our considerations. The goal of the present paper is to introduce an alternative regularization concept into the application field of optical flow estimation. In the ill-posed problems community, Natterer proved in [31] that projection methods have a regularizing effect, see also Louis [23]. Although such a regularizing effect has also been mentioned by Szeliski and Coughlan in a paper on spline-based image registration [39], a mathematical investigation of projection methods for optical flow estimation is missing so far. In the present work we address this problem. The idea is to minimize a functional in a finite dimensional, affine subspace. Thus, the resulting optical flow field is uniquely determined as solution of a system of equations and has any desired properties if we only choose the subspace and the corresponding basis functions properly. In order to make the basic principles as clear as possible, we stick to relatively simple optical flow assumptions. Thus, our goal is rather to introduce a new direction of optical flow methods than to compete with the current state-of-the-art. Projection methods offer a number of properties that might be appealing in the optical flow context, for example regularity estimates or the flexibility to incorporate certain constraints in an elegant way. In the area of inverse problems projection methods are also used to get asymptotic error estimates for solvers as e.g. in the article of Rieder and Schuster [34].

Our paper is organized as follows. In section 2 we give a short description of general variational approaches for optical flow computation. Section 3 outlines how projection methods can be used to solve the variation problem, where the energy functional to be minimized essentially consists of the data term. We present ideas how to solve the arising system of linear or nonlinear equations. In section 4 we prove that the residual error always is optimal in the sense that the error is bounded by a multiple of the approximation module of the applied basis functions. In case of the application of tensor product B-splines we are able to present the convergence rates explicitly. Finally section 5 contains some numerical experiments with tensor products of piecewise linear splines which show the performance of the method. The paper is concluded with a summary in section 6.

2 Variational computation of optical flow

Let $\Omega \subset \mathbb{R}^2$ denote a rectangular image domain. We assume that a sequence of images

$$f(x_1, x_2, t)\,, \qquad (x_1, x_2) \in \Omega\,, \quad t \in [0, T]$$

is given, where $f(x_1, x_2, t)$ denotes the gray value of the pixel $\mathbf{x} = (x_1, x_2)$ at time t. Recovering the *optical flow field* $\mathbf{u} = (u_1(x_1, x_2, t), u_2(x_1, x_2, t), 1)^\top$ means to find the apparent velocity

$$(u_1, u_2)^\top = \left(\frac{\partial x_1}{\partial t}, \frac{\partial x_2}{\partial t}\right)^\top$$

of a structure that moves along its trajectory $(x_1(t), x_2(t))^\top$. Many optical flow computations are based on the so-called *optical flow constraint* that assumes that the gray value of a pixel does not change over time. In this case we have

$$0 = \frac{df(x_1(t), x_2(t), t)}{dt} = f_{x_1} u_1 + f_{x_2} u_2 + f_t = \langle \mathbf{u}, \nabla f \rangle\,, \tag{1}$$

where $\nabla := (\partial_{x_1}, \partial_{x_2}, \partial_t)$ denotes the spatiotemporal nabla operator. Obviously the optical flow constraint (1) is not sufficient for a full reconstruction of $\mathbf{u}$. Thus, one furthermore postulates smoothness conditions for $\mathbf{u}$. In general, variational optical flow computation with a spatiotemporal smoothness constraint aims at minimizing an energy functional $E(\mathbf{u})$ of the form

$$E(\mathbf{u}) = \int_0^T \int_\Omega \Big(M(D^k f, \mathbf{u}) + \alpha\, S(\nabla f, \nabla \mathbf{u}) \Big)\, \mathrm{d}x\, \mathrm{d}t\,. \tag{2}$$

The expression $M(D^k f, \mathbf{u})$ involves a k-th order differential operator $D^k f$ of f and $\mathbf{u}$ and is called *data term*. It is connected to conservation assumptions such as the optical flow constraint. A simple and obvious choice would be $M(D^1 f, \mathbf{u}) = \langle \mathbf{u}, \nabla f \rangle^2$. To get uniqueness a *regularization term* $S(\nabla f, \nabla \mathbf{u})$ is added which also guarantees smoothness of the optical flow field $\mathbf{u}$. In that sense α can be seen as a regularization parameter. The regularizer $S(\nabla f, \nabla \mathbf{u})$ also causes *filling-in effects*. In regions with almost constant gray values, the data term is rather small and $E(\mathbf{u})$ is dominated by the smoothness term which fills in information from other locations. Thus, no further interpolation is necessary. We refer to Horn and Schunck [20] for this topic. A list of different data and regularization terms can be found in Weickert et al. [41].

So far we have not assumed any smoothnes conditions for f and $\mathbf{u}$. In view of (1) f has to be at least differentiable. The smoothness assumptions also depend on the particular choice of M and S in (2). We will specify the smoothness conditions in section 4.

Subject of variational optical flow computation is the global minimization of $E(\mathbf{u})$. If E is convex, then there exists a global minimum which we denote by $\mathbf{u}^*$. Very efficient methods to calculate $\mathbf{u}^*$ numerically can be achieved by discretizing the Euler–Lagrange equation associated to E and a subsequent solution of the arising system of linear or nonlinear equations by multigrid methods. These techniques are amongst the most accurate solvers for optical flow problems; see e.g. [18, 17, 43, 9, 27, 13].

3 Projection methods for solving the minimization problem

Let us now present a novel variational approach for optical flow estimation using projection methods. Instead of minimizing E we consider the functional

$$E_\Psi(\mathbf{u}) = \frac{1}{2} \int_0^T \int_\Omega \Psi\Big(\langle \mathbf{u}, \nabla f \rangle^2\Big) \, \mathrm{d}x \, \mathrm{d}t \tag{3}$$

for an *admissible* function Ψ. A strictly increasing function Ψ is admissible if $\Psi \in \mathcal{C}^2([0, +\infty))$ and $\Psi(s^2)$ is convex in s. The functional E_Ψ is convex for admissible Ψ and hence has a unique minimizer which we again denote by $\mathbf{u}^*$. The simplest choice of an admissible Ψ is $\Psi(t) = t$ leading to quadratic minimization problems, but also nonquadratic approaches such as $\Psi(t) = \sqrt{\epsilon + t}$ with $\epsilon > 0$ are possible in order to obtain higher robustness against outliers [21]. Such robust strategies are frequent in optical flow estimation; see e.g. [5, 8, 19, 26].

The idea behind projection methods is as follows: We search for a solution $\mathbf{u}_n^* = ((u_n^*)_1, (u_n^*)_2, 1)$ in a finite dimensional, affine space $V_n = e_3 \oplus \widetilde{V}_n$, where $\widetilde{V}_n$ is a linear subspace of $L^p(\Omega, \mathbb{R}^3)$ with $\dim \widetilde{V}_n = d_n < \infty$ and $1 \leq p \leq +\infty$. We define

$$\mathbf{u}_n^* := \arg\min_{\mathbf{v} \in V_n} E_\Psi(\mathbf{v}) . \tag{4}$$

In order to get a meaningful solution and to yield convergence results for $n \to \infty$, the union of the linear subspaces $\widetilde{V}_n$ is supposed to be dense. To be precise,

$$\overline{\bigcup_{n=1}^{\infty} \widetilde{V}_n} = (L^p(\Omega, \mathbb{R}^3) \cap \{e_3^\perp\} . \tag{5}$$

Since $\widetilde{V}_n$ is a finite dimensional subspace, there is a basis $\{\phi_1^n, \dots, \phi_n^n\}$ with $\widetilde{V}_n = \text{span } \{\phi_1^n, \dots, \phi_n^n\}$. To solve problem (4) we use the expansion

$$\mathbf{u}_n^* = e_3 + \sum_{n=1}^{n} \beta_i^* \, \phi_i^n \tag{6}$$

to get a minimization problem over $\mathbb{R}^n$:

$$\min_{\mathbf{v} \in V_n} E_\Psi(\mathbf{v}) = \min_{\beta \in \mathbb{R}^n} \frac{1}{2} \int_0^T \int_\Omega \Psi\Big((\langle e_3 + \sum_{i=1}^{n} \beta_i \, \phi_i^n, \nabla f \rangle)^2\Big) \, \mathrm{d}x \, \mathrm{d}t \, .$$

For the sake of simplicity we also write $E_\Psi(\beta)$ for $\beta \in \mathbb{R}^n$ instead of $E_\Psi(\mathbf{v})$ for $\mathbf{v} \in V_n$. We set

$$\beta^* := \arg\min_{\beta \in \mathbb{R}^n} E_\Psi(\beta)$$

and compute β^* by solving

$$\nabla E_\Psi(\beta^*) = 0 \, . \tag{7}$$

We will see that this can be done by applying direct methods or iterative techniques such as the Newton method. The case $\Psi(s^2) = s^2$ plays a particular role since here β^* can be described as solution of a system of linear equations.

Remark 3.1 *Natterer proved in* [31] *that projection methods have a regularizing effect and that is why we have no additional smoothing term in* (3). *Furthermore we only consider the spatial approach for optical flow computation, that means our searched approximation* $\mathbf{u}_n^*$ *does not depend on the time* t. *That is why there is no temporal variable in* $\widetilde{V}_n \subset L^p(\Omega, \mathbb{R}^3)$.

3.1 The case $\Psi(t) = t$

For $\Psi(t) = t$ we compute

$$\frac{\partial E_\Psi(\beta)}{\partial \beta_j} = \int\limits_0^T \int_\Omega \Big\{ (f_t + \sum_{i=1}^n \beta_i \langle \phi_i^n, \nabla f \rangle) \langle \phi_j^n, \nabla f \rangle \Big\} \,\mathrm{d}x \,\mathrm{d}t \,, \tag{8}$$

$j = 1, \ldots, n$. Hence, (7) is equivalent to solving the system of linear equations $\mathbf{A}\beta^* = \mathbf{b}$ with

$$\mathbf{A}_{jj'} = \int\limits_0^T \int_\Omega \langle \phi_j^n, \nabla f \rangle \langle \phi_{j'}^n, \nabla f \rangle \,\mathrm{d}x \,\mathrm{d}t \,, \qquad 1 \leq j, j' \leq n$$

and

$$\mathbf{b}_j = -\int\limits_0^T \int_\Omega f_t \langle \phi_j^n, \nabla f \rangle \,\mathrm{d}x \,, \qquad 1 \leq j \leq n \,.$$

Since

$$\langle \beta, \mathbf{A}\beta \rangle = \sum_{j=1}^n \beta_j^2 \int\limits_0^T \int_\Omega \langle \phi_j^n, \nabla f \rangle^2 \,\mathrm{d}x \,\mathrm{d}t \geq 0 \,, \qquad \beta \in \mathbb{R}^n \,,$$

the matrix $\mathbf{A}$ is symmetric and positiv semidefinite. If we use basis functions ϕ_i^n with small, compact support, $\mathbf{A}$ furthermore is sparse and thus iterative solvers as the CG- or CGS-method are appropriate for solving the system. The choice $\Psi(t) = t$ is the case which we will study thoroughly in section 4. There, we will use tensor product B-splines which have all the desired properties and which are also used for the numerical experiments in section 5. The projection method to solve the variational optical flow problem in case $\Psi(t) = t$ finally reads as follows:

- Choose a linear, finite dimensional subspace $\widetilde{V}_n$ and an appropriate basis $\{\phi_1^n, \ldots, \phi_n^n\}$.
- Compute $\mathbf{A}$ and $\mathbf{b}$, e.g. by using numerical integration.
- Solve $\mathbf{A}\beta^* = \mathbf{b}$, e.g. by iterative solvers such as CG or CGS [35].
- Compute

$$\mathbf{u}_n^* = e_3 + \sum_{n=1}^n \beta_i^* \, \phi_i^n \,.$$

3.2 The case, where Ψ is an arbitrary, admissible function

For arbitrary Ψ equation (7) represents a system of nonlinear equations. Such systems can be solved e.g. by Newton's method. The gradient and Hesse matrix of E_Ψ read

$$
\begin{aligned}
\frac{\partial E_\Psi(\beta)}{\partial \beta_j} &= \\
&\int_0^T \int_\Omega \Big\{ \Psi'\Big((f_t + \sum_{i=1}^n \beta_i \langle \phi_i^n, \nabla f \rangle)^2 \Big) (f_t + \sum_{i=1}^n \beta_i \langle \phi_i^n, \nabla f \rangle) \langle \phi_j^n, \nabla f \rangle \Big\} \mathrm{d}x \, \mathrm{d}t \,,
\end{aligned}
$$

$$
\begin{aligned}
\frac{\partial^2 E_\Psi(\beta)}{\partial \beta_j \, \partial \beta_{j'}} &= 2 \int_0^T \int_\Omega \Big\{ \Psi''\Big((f_t + \sum_{i=1}^n \beta_i \langle \phi_i^n, \nabla f \rangle)^2 \Big) \times \\
&\qquad (f_t + \sum_{i=1}^n \beta_i \langle \phi_i^n, \nabla f \rangle)^2 \langle \phi_j^n, \nabla f \rangle \langle \phi_{j'}^n, \nabla f \rangle \Big\} \, \mathrm{d}x \, \mathrm{d}t \\
&+ \int_0^T \int_\Omega \Big\{ \Psi'\Big((f_t + \sum_{i=1}^n \beta_i \langle \Phi_i, \nabla f \rangle)^2 \Big) \langle \Phi_j, \nabla f \rangle \langle \Phi_{j'}, \nabla f \rangle \Big\} \, \mathrm{d}x \, \mathrm{d}t \,,
\end{aligned}
$$

where $1 \leq j, j' \leq n$. The system of nonlinear equations (7) can be solved numerically by the Newton method: Choose an initial guess $\beta^{(0)} \in \mathbb{R}^n$ and iterate

$$\beta^{(k+1)} = \beta^{(k)} + \delta\beta^{(k)} \,, \qquad k = 0, 1, 2, \ldots$$

where $\delta\beta^{(k)}$ solves

$$\nabla^2 E_\Psi(\beta^{(k)}) \delta\beta^{(k)} = -\nabla E_\Psi(\beta^{(k)}) \,.$$

3.3 More general data terms

We observe that the functional (3) may also be written as

$$E_\Psi(\mathbf{u}) = \frac{1}{2} \int_0^T \int_\Omega \Psi\Big(\langle \mathbf{u}, \mathbf{J}_f \mathbf{u} \rangle \Big) \, \mathrm{d}x \, \mathrm{d}t \tag{9}$$

with the structure tensor $\mathbf{J}_f = \nabla f \otimes \nabla f$. Defining E_Ψ as in (9) for a symmetric tensor field $\mathbf{J}_f$ of rank 2 related to f and defined on $\Omega \times [0, T]$ we can also apply more general data terms. For instance, instead of the optical flow constraint $\langle \mathbf{u}, \nabla f \rangle = 0$ we could assume constancy of the brightness gradient [40] leading to

$$\mathbf{J}_f = \sum_{i=1}^{2} (\nabla f_{x_i} \otimes \nabla f_{x_i}) \,. \tag{10}$$

Again using expansion (6) we find for $\Psi(t) = t$ that

$$\frac{\partial E_\Psi(\beta)}{\partial \beta_j} = \int_0^T \int_\Omega \Big\{ \langle e_3, \mathbf{J}_f \phi_j^n \rangle + \sum_{i=1}^{n} \beta_i \langle \phi_i^n, \mathbf{J}_f \phi_j^n \rangle \Big\} \,\mathrm{d}x \,\mathrm{d}t \,, \tag{11}$$

$j = 1, \ldots, n$. This results in the system of linear equations $\mathbf{A}\beta^* = \mathbf{b}$ with

$$\mathbf{A}_{jj'} = \int_0^T \int_\Omega \langle \phi_j^n, \mathbf{J}_f \phi_{j'}^n \rangle \,\mathrm{d}x \,\mathrm{d}t \,, \qquad 1 \leq j, j' \leq n$$

and

$$\mathbf{b}_j = -\int_0^T \int_\Omega \langle e_3, \mathbf{J}_f \phi_j^n \rangle \,\mathrm{d}x \,, \qquad 1 \leq j \leq n \,.$$

Note that $\mathbf{A}$ remains positive semidefinite, since $\mathbf{J}_f$ was supposed to be symmetric. A lot of different data terms can be involved in that way. We again refer to [41] for an overview of various constancy assumptions.

4 Convergence rates for tensor product B-splines and $\Psi(t) = t$

In this section we investigate the deviation of the projected solution $\mathbf{u}_n^*$ from the global minimizer $\mathbf{u}^*$ of E_Ψ, where $\Psi(t) = t$ and $\mathbf{J}_f = \nabla f \otimes \nabla f$. Particularly we will use tensor product B-splines of arbitrary order m as basis functions ϕ_i and show optimal convergence with respect to the residual. To this end we first prove continuity of E_Ψ in $L^p(\Omega, \mathbb{R}^3)$ for all $2 \leq p \leq \infty$, if the image sequence f satisfies certain smoothness conditions. These conditions are expressed by means of the Sobolev spaces $W^{\alpha,p}(\Omega \times [0,T])$, $\alpha \geq 0$. They consist of functions $f \in L^p(\Omega \times [0,T])$ which have weak derivatives in $L^p(\Omega \times [0,T])$ up to the order α. For integers α and $2 \leq p < \infty$ the norm is given as

$$\|\mathbf{u}\|_{\alpha,p} = \Big(\int_0^T \int_\Omega \sum_{|k| \leq \alpha} \|D^k \mathbf{u}(x,t)\|_2^p \,\mathrm{d}x \,\mathrm{d}t \Big)^{1/p} ,$$

where $k \in \mathbb{N}_0^3$ is a multi-index. For $p = \infty$ and integer α we have

$$\|\mathbf{u}\|_{\alpha,\infty} = \max_{|k|\leq\alpha} \|D^k \mathbf{u}\|_\infty .$$

We have that $W^{\alpha,2} = H^\alpha$. For a detailed treatise of Sobolev spaces we refer to Maz'ja [25].

Lemma 4.1 (Continuity of E_Ψ)
Let $\Psi(t) = t$. The functional $E_\Psi : L^p(\Omega, \mathbb{R}^3) \to [0, +\infty)$ is continuous for any $2 \leq p \leq \infty$, if f satisfies

- $f \in W^{1,2q'}(\Omega \times [0,T])$, $(q')^{-1} + (p')^{-1} = 1$, $p' = p/2$ *in case* $2 < p < \infty$
- $f \in W^{1,\infty}(\Omega \times [0,T])$ *in case* $p = 2$
- $f \in W^{1,2}(\Omega \times [0,T])$ *in case* $p = \infty$

More explicitly, under these smoothness conditions for f there exists a constant $C_p > 0$ such that

$$|E_\Psi(\mathbf{u})| \leq C_p \|\mathbf{u}\|_p^2 , \qquad \mathbf{u} \in L^p(\Omega, \mathbb{R}^3) . \tag{12}$$

Proof: Obviously the boundedness estimate (12) implies the continuity of E_Ψ, hence it is sufficient to prove (12). For $\Psi(t) = t$ and $\mathbf{u} \in L^p(\Omega, \mathbb{R}^3)$ we have

$$\begin{aligned} |E_\Psi(\mathbf{u})| &\leq \frac{1}{2} \int_0^T \int_\Omega |\langle \mathbf{u}(x), \nabla f(x,t) \rangle|^2 \,\mathrm{d}x\,\mathrm{d}t \\ &\leq \frac{1}{2} \int_0^T \int_\Omega \|\mathbf{u}(x)\|_2^2 \,\|\nabla f(x,t)\|_2^2 \,\mathrm{d}x\,\mathrm{d}t \end{aligned}$$

by the Cauchy-Schwartz inequality. To continue we take into account the smoothness conditions for f as listed in the theorem. Note that all these conditions imply the existence of ∇f.
In case $p = 2$ we postulate $f \in W^{1,\infty}(\Omega \times [0,T])$ and thus

$$|E_\Psi(\mathbf{u})| \leq \frac{1}{2} T \|f\|_{1,\infty}^2 \int_\Omega \|\mathbf{u}(x)\|_2^2 \,\mathrm{d}x ,$$

which yields (12) with $C_p := T\|f\|_{1,\infty}^2/2$.
In case $p = \infty$ we have that $f \in W^{1,2}(\Omega \times [0,T])$ and immediately obtain

$$|E_\Psi(\mathbf{u})| \leq \frac{1}{2} \|f\|_{1,2}^2 \|\mathbf{u}\|_\infty^2$$

and therefore $C_p := \|f\|_{1,2}^2/2$ in (12).
For all other p with $2 < p < \infty$ we use the Hölder inequality. Define $p' := p/2$ and let q' the reciprocal of p', that is the unique number q' satisfying $1/p' + 1/q' = 1$. An application of the Hölder inequality gives

$$\begin{aligned} |E_\Psi(\mathbf{u})| &\leq \frac{1}{2}\Bigg(\int\limits_0^T \int_\Omega \|\mathbf{u}\|_2^{2p'} \,\mathrm{d}x\,\mathrm{d}t\Bigg)^{1/p'} \Bigg(\int\limits_0^T \int_\Omega \|\nabla f\|_2^{2q'} \,\mathrm{d}x\,\mathrm{d}t\Bigg)^{1/q'} \\ &= \frac{1}{2}\,T^{2/p}\,\|f\|_{1,2q'}^2 \Bigg(\int_\Omega \|\mathbf{u}\|_2^p \,\mathrm{d}x\Bigg)^{2/p} \end{aligned}$$

and we again obtain (12), where $C_p := T^{2/p}\|f\|_{1,2q'}^2/2$ in this case. □

Under the smoothness conditions of lemma 4.1 the functional E_Ψ is Fréchet differentiable.

Lemma 4.2 (Fréchet-differentiability of E_Ψ)
Adopt the assumptions made in lemma 4.1. Then $E_\Psi : L^p(\Omega, \mathbb{R}^3) \to \mathbb{R}$ is Fréchet-differentiable for $\Psi(t) = t$. The Fréchet-derivative $E'_\Psi : L^p(\Omega, \mathbb{R}^3) \to \mathcal{L}(L^p(\Omega, \mathbb{R}^3), \mathbb{R})$ is given by

$$E'_\Psi(\mathbf{u})\mathbf{v} = \int\limits_{\mathbf{0}}^{\mathbf{T}} \int_{\mathbf{\Omega}} \langle \mathbf{u}, \nabla \mathbf{f}\rangle \,\langle \mathbf{v}, \nabla \mathbf{f}\rangle \,\mathrm{d}\mathbf{x}\,\mathrm{d}\mathbf{t}\,, \qquad \mathbf{u}, \mathbf{v} \in \mathbf{L^p}(\mathbf{\Omega}, \mathbb{R}^{\mathbf{3}})\,.$$

Especially for $\mathbf{v} = \mathbf{u}$ we have

$$E'_\Psi(\mathbf{u})\mathbf{u} = 2\,E_\Psi(\mathbf{u})\,, \qquad \mathbf{u} \in L^p(\Omega, \mathbb{R}^3)\,. \tag{13}$$

Proof: Let $\mathbf{v} \in \mathcal{C}_0^\infty(\Omega, \mathbb{R}^3)$. We compute

$$\begin{aligned} \frac{\partial E_\Psi(\mathbf{u} + \tau\,\mathbf{v})}{\partial \tau}_{|\tau=0} &= \frac{1}{2}\Bigg\{\frac{\partial}{\partial \tau}\int\limits_0^T \int_\Omega \langle \mathbf{u} + \tau\,\mathbf{v}, \nabla f\rangle^2 \,\mathrm{d}x\,\mathrm{d}t\Bigg\}_{|\tau=0} \\ &= \Bigg\{\int\limits_0^T \int_\Omega \langle \mathbf{u}, \nabla f\rangle\,\langle \mathbf{v}, \nabla f\rangle \,\mathrm{d}x\,\mathrm{d}t + \tau \int\limits_0^T \int_\Omega \langle \mathbf{v}, \nabla f\rangle^2 \,\mathrm{d}x\,\mathrm{d}t\Bigg\}_{|\tau=0} \\ &= \int\limits_0^T \int_\Omega \langle \mathbf{u}, \nabla f\rangle\,\langle \mathbf{v}, \nabla f\rangle \,\mathrm{d}x\,\mathrm{d}t =: E'_\Psi(\mathbf{u})\mathbf{v}\,. \end{aligned}$$

To prove that this in fact is the Fréchet derivative we verify that

$$\begin{aligned}
\lim_{\|\mathbf{v}\|_p \to 0} & \frac{\|E_\Psi(\mathbf{u}+\mathbf{v}) - E_\Psi(\mathbf{v}) - E'_\Psi(\mathbf{u})\mathbf{v}\|_p}{\|\mathbf{v}\|_p} \\
&= \lim_{\|\mathbf{v}\|_p \to 0} \|\mathbf{v}\|_p^{-1} \int_0^T \int_\Omega \langle \mathbf{v}, \nabla f \rangle^2 \, \mathrm{d}x \, \mathrm{d}t \\
&\leq \lim_{\|\mathbf{v}\|_p \to 0} C_p \, \|\mathbf{v}\|_p = 0 \,,
\end{aligned}$$

where we used (12). $\square$

Remark 4.3 *By appropriate Taylor expansions one can easily show that* E_Ψ *is Fréchet-differentiable for all admissible* Ψ *with*

$$E'_\Psi(\mathbf{u})\mathbf{v} = \int_0^T \int_\Omega \Psi'(\langle \mathbf{u}, \nabla f \rangle^2) \, \langle \mathbf{u}, \nabla f \rangle \, \langle \mathbf{v}, \nabla f \rangle \, \mathrm{d}x \, \mathrm{d}t \,, \qquad \mathbf{u}, \mathbf{v} \in L^p(\Omega, \mathbb{R}^3) \,.$$

By now we did not specify the linear subspace $\widetilde{V}_n \subset L^p(\Omega, \mathbb{R}^3)$ and the basis functions $\{\phi_1^n, \ldots, \phi_n^n\}$. To get a sparse matrix $\mathbf{A}$ we want the functions ϕ_i^n to be compactly supported. On the other hand they are supposed to have good approximation properties and to be smooth to yield a smooth flow field. B-splines satisfy all these conditions. To construct the set of knots associated to the B-splines we set $\Omega := [0,1]^2$ and assume $f(x_1, x_2, t)$ to be given for

$$(x_1^{(j)}, x_2^{(j')}) = \Big((j-1)/d, (j'-1)/d \Big) \,, \qquad 1 \leq j, j' \leq d \,, \tag{14}$$

where d^2 represents the number of pixels. The *B-spline of order* m corresponding to the knots $\{x_1^{(j)}\}$ is recursively defined as

$$N_j^m(x) = (x - x_1^{(j)}) \, N_j^{m-1}(x) + (x_1^{(j+m)} - x) \, N_{j+1}^{m-1}(x) \qquad m \geq 2$$

and

$$N_j^1(x) = \begin{cases} 1 \,, & x_1^{(j)} \leq x \leq x_1^{(j+1)} \\ 0 \,, & \text{otherwise} \end{cases}$$

We have that $N_j^m \in \mathcal{C}^{m-2}([0,1])$ and $\operatorname{supp} N_j^m = [x_1^{(j)}, x_1^{(j+m)}]$. Moreover, the B-splines form a partition of unity. A detailed outline of the construction and properties of B-splines are found in the book of Schumaker [37]. Note that our knot sequences $x_1^{(j)}$, $x_2^{(j')}$ are equidistant with step size d^{-1}. With the help of N_j^m we define the basis of the linear subspace. For $1 \le j, j' \le d$ and $m \ge 1$ let

$$\phi_{j,j'}^{(\nu),m}(x_1, x_2) := (N_j^m \otimes N_{j'}^m)(x_1, x_2) \cdot e_\nu \qquad \nu = 1, 2\,,$$

where $N_{j'}^m$ denotes the B-spline of order m associated to the knots $\{x_2^{(j')}\}$ and e_ν are the standard unit vectors in $\mathbb{R}^3$. E.g.

$$\phi_{j,j'}^{(1),m} = (N_j^m \otimes N_{j'}^m, 0, 0)\,.$$

Finally we define the linear subspace $\widetilde{V}_n$ as

$$\begin{aligned} \widetilde{V}_n := W_d^m \;&:=\; \operatorname{span}\left\{\phi_{j,j'}^{(\nu),m} : \nu = 1, 2\,,\ 1 \le j, j' \le d + m - 2\right\} \\ &\subset\; \left(L^p(\Omega, \mathbb{R}^3) \cap \{e_3^\perp\}\right). \end{aligned}$$

The linear subspace W_d^m is generated by tensor product B-splines and we have $\dim W_d^m = 2(d + m - 2)^2$. Figure 1 shows a B-spline of order 2, which is a piecewise, linear spline and a graphic of a tensor product B-spline.

To make the notation clear we state three minimizing solutions of different kind. Again

$$\mathbf{u}^* := \arg\min\{E_\Psi(\mathbf{u}) : \mathbf{u} = e_3 + L^p(\Omega, \mathbb{R}^3)\}$$

is the global minimizer. Corresponding to the space W_d^m

$$\mathbf{u}_{d,m}^* := \arg\min\{E_\Psi(\mathbf{u}) : \mathbf{u} = e_3 + W_d^m\}$$

means the solution in the finite dimensional, affine space $e_3 + W_d^m$, which was formerly denoted by $\mathbf{u}_n^*$. At last

$$\tilde{\mathbf{u}}_{d,m}^* := \arg\min\{\|\mathbf{u}^* - \mathbf{u}\|_p : \mathbf{u} \in e_3 + W_d^m\}$$

is the best approximation of $\mathbf{u}^*$ in $e_3 + W_d^m$. Our aim is to find an estimate for the error

$$|E_\Psi(\mathbf{u}^*) - E_\Psi(\mathbf{u}_{d,m}^*)|\,. \tag{15}$$

We recall that $\Psi(t) = t$ in our considerations. From the approximation theory of tensor product B-splines we know that

$$\|\mathbf{u}^* - \tilde{\mathbf{u}}_{d,m}^*\|_p \le K\, d^{-\min\{\alpha, m\}}\, \|\mathbf{u}^*\|_{\alpha,p}\,, \tag{16}$$

if $\mathbf{u} \in W^{\alpha,p}(\Omega, \mathbb{R}^3)$ for a constant $K > 0$, see Schumaker [37, Chapter 12.3]. The main result of this section consists of the proof that the error (15) has a convergence of the same order as in (16).

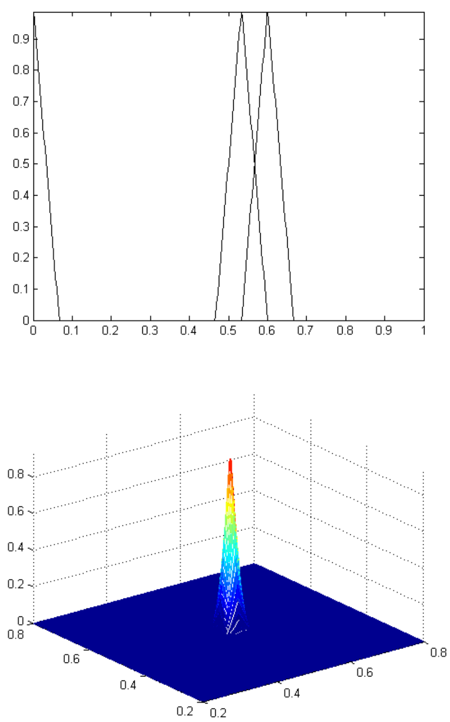

Figure 1: B-splines of order 2 (left picture) and a tensor product B-spline $N_j^2 \otimes N_{j'}^2$ (right picture).

Theorem 4.4 (Estimate of the residual error)
Adopt all notations made so far as well as the smoothness assumptions for f stated in lemma 4.1. Let $\Psi(t) = t$. If $\mathbf{u}^* \in W^{\alpha,p}(\Omega, \mathbb{R}^3)$ for $\alpha \geq 0$ and $2 \leq p \leq \infty$, then there exists a constant $K_p > 0$ such that

$$|E_\Psi(\mathbf{u}^*) - E_\Psi(\mathbf{u}^*_{d,m})| \leq K_p\, d^{-\min\{\alpha,m\}}\, \|\mathbf{u}^*\|_{\alpha,p}\,. \tag{17}$$

Furthermore we have $\mathbf{u}^*_{d,m} \in \mathcal{C}^{m-2}(\Omega, \mathbb{R}^3)$.

Proof: First we show that there exists a constant $M_p > 0$ satisfying

$$\|E'_\Psi(\mathbf{u})\|_{L^p \to \mathbb{R}} \leq M_p\, \|\mathbf{u}\|_p\,, \tag{18}$$

if $\mathbf{u} \in L^p(\Omega, \mathbb{R}^3)$. Assertion (18) results from

$$\begin{aligned}
\|E'_\Psi(\mathbf{u})\|_{L^p\to\mathbb{R}} &= \sup_{\|\mathbf{v}\|_p \leq 1} \Big| \int_0^T \int_\Omega \langle \mathbf{u}, \nabla f\rangle\, \langle \mathbf{v}, \nabla f\rangle\, \mathrm{d}x\, \mathrm{d}t \Big| \\
&\leq \sup_{\|\mathbf{v}\|_p \leq 1} \Big(\int_0^T \int_\Omega \langle \mathbf{v}, \nabla f\rangle^2\, \mathrm{d}x\, \mathrm{d}t \Big)^{1/2} \Big(\int_0^T \int_\Omega \langle \mathbf{u}, \nabla f\rangle^2\, \mathrm{d}x\, \mathrm{d}t \Big)^{1/2} \\
&\leq \sup_{\|\mathbf{v}\|_p \leq 1} \sqrt{2E_\Psi(\mathbf{v})}\, \sqrt{2E_\Psi(\mathbf{u})} \leq \sqrt{2C_p}\, \sqrt{2C_p}\, \|\mathbf{u}\|_p
\end{aligned}$$

setting $M_p := 2C_p$. Here, we used (12). By construction we have that

$$0 \leq E_\Psi(\mathbf{u}^*) \leq E_\Psi(\mathbf{u}^*_{d,m}) \leq E_\Psi(\tilde{\mathbf{u}}^*_{d,m})\,. \tag{19}$$

From (16) we know that $\tilde{\mathbf{u}}^*_{d,m} \to \mathbf{u}^*$ as $d \to \infty$ and thus

$$\|\tilde{\mathbf{u}}^*_{d,m}\|_p \leq C\,, \qquad d > 0 \tag{20}$$

for a certain $C > 0$. Furthermore, if we use the fact that E'_Ψ is linear as mapping between $L^p(\Omega, \mathbb{R}^3)$ and $\mathcal{L}(L^p(\Omega, \mathbb{R}^3), \mathbb{R})$, then putting together (13), (18), (19) and (20) yields

$$\begin{aligned}
|E_\Psi(\mathbf{u}^*) - E_\Psi(\mathbf{u}^*_{d,m})| &\leq |E_\Psi(\mathbf{u}^*) - E_\Psi(\tilde{\mathbf{u}}^*_{d,m})| \\
&\leq \left| \frac{1}{2} E'_\Psi(\mathbf{u}^*)(\mathbf{u}^* - \tilde{\mathbf{u}}^*_{d,m}) \right| + \left| \frac{1}{2} E'_\Psi(\mathbf{u}^* - \tilde{\mathbf{u}}^*_{d,m}) \tilde{\mathbf{u}}^*_{d,m} \right| \\
&\leq \frac{1}{2} \|E'_\Psi(\mathbf{u}^*)\|_{L^p\to\mathbb{R}}\, \|\mathbf{u}^* - \tilde{\mathbf{u}}^*_{d,m}\|_p + \frac{1}{2} \|E'_\Psi(\mathbf{u}^* - \tilde{\mathbf{u}}^*_{d,m})\|_{L^p\to\mathbb{R}}\, \|\tilde{\mathbf{u}}^*_{d,m}\|_p \\
&\leq \frac{1}{2} M_p\, (\|\mathbf{u}^*\|_p + C)\, \|\mathbf{u}^* - \tilde{\mathbf{u}}^*_{d,m}\|_p\,,
\end{aligned}$$

what proves (17) with $K_p := M_p(\|\mathbf{u}^*\|_p + C)/2$.
The smoothness statement is obvious, since $\mathbf{u}^*_{d,m}$ is a finite sum of vector fields having components which consist of tensor product B-splines of this very regularity. $\square$

Remark 4.5 *Theorem* 4.4 *on the one hand shows why we could omit the regularization term in the functional E_Ψ. Since the solution is a finite sum of smooth functions, it has the same regularity as the basis functions. On the other hand the residual error $|E_\Psi(\mathbf{u}^*) - E_\Psi(\mathbf{u}^*_{d,m})|$ tends to zero as $d \to \infty$ of the same order as the approximation module of the applied B-splines. In that sense we say that the projection method has optimal convergence rate when using B-splines. A further advantage is the small support of the splines which yields a sparse system matrix $\mathbf{A}$. Thus, the arising system of linear equations $\mathbf{A}\beta^* = \mathbf{b}$ can be solved iteratively, e.g. by the CG-method.*

A look at the proof of theorem 4.4 shows that the residual error $|E_\Psi(\mathbf{u}^*) - E_\Psi(\mathbf{u}^*_n)|$ is always of the same order as the approximation power of the applied basis functions, since that error can be bounded by a multiple of $\|\mathbf{u} - \mathbf{u}^*_n\|$.

Corollary 4.6 *Adopt the notations from section* 3 *and the smoothness assumptions for f listed in lemma* 4.1*. Let $\Psi(t) = t$. Further suppose that* (5) *is satisfied. Then, the residual error $|E_\Psi(\mathbf{u}^*) - E_\Psi(\mathbf{u}^*_n)|$ is of the same order as the approximation module of $\widetilde{V}_n$.*

Proof: This statement follows from the proof of theorem 4.4. The last estimate in this proof is still valid if we replace the special approximation $\tilde{\mathbf{u}}^*_{d,m}$ by $e_3 + P_n(\mathbf{u}^* - e_3)$, where $P_n : L^p(\Omega, \mathbb{R}^3) \to \widetilde{V}_n$ is the orthogonal projection onto $\widetilde{V}_n$. That means that $|E_\Psi(\mathbf{u}^*) - E_\Psi(\mathbf{u}^*_n)|$ is bounded by a multiple of $\|\mathbf{u}^* - (e_3 + P_n(\mathbf{u}^* - e_3))\|_p$. This factor tends to 0 for $n \to \infty$ by (5) and describes the approximation module of $\widetilde{V}_n$. $\square$

5 Numerical experiments

We perform the method described in section 3.1 by means of several test sequences using the classical optical flow constraint with $J_f = \nabla f \otimes \nabla f$ as well as the gradient constancy assumption with (10). In all experiments we chose $\Psi(t) = t$. As basis functions we use piecewise linear tensor product B-splines associated with the knots $\{x_1^{(j)}\}$, $\{x_2^{(j')}\}$ from (14),

$$\phi_{j,j'}^{(\nu),2}(x_1, x_2) := (N_j^2 \otimes N_{j'}^2)(x_1, x_2) \cdot e_\nu \,, \qquad \nu = 1, 2 \tag{21}$$

which span the linear subspace

$$W_d^2 = \operatorname{span}\left\{\phi_{j,j'}^{(\nu),2} : \nu = 1, 2\,,\ 1 \le j, j' \le d\right\}$$

of dimension $2d^2$.

5.1 The classical optical flow constraint

For an image sequence $f(x_1, x_2, t)$ we have to solve the system $\mathbf{A}\beta^* = \mathbf{b}$, where $\mathbf{A} \in \mathbb{R}^{2d^2 \times 2d^2}$, $\mathbf{b} \in \mathbb{R}^{2d^2}$ are given as

$$\begin{aligned} \mathbf{A}_{(jj'),(kk')}^{(\nu\mu)} &= \int_0^T \int_\Omega \langle \phi_{j,j'}^{(\nu),2}, \nabla f\rangle \, \langle \phi_{k,k'}^{(\mu),2}, \nabla f\rangle \, \mathrm{d}x \, \mathrm{d}t \qquad (22) \\ &= \int_0^T \int_\Omega f_{x_\nu}(x_1, x_2, t)\, N_j^2(x_1)\, N_{j'}^2(x_2)\, f_{x_\mu}(x_1, x_2, t)\, N_k^2(x_1)\, N_{k'}^2(x_2)\, \mathrm{d}x\, \mathrm{d}t \,, \end{aligned}$$

where $1 \le \nu, \mu \le 2$ and $1 \le j, j', k, k' \le d$, compare subsection 3.1. Note that $\mathbf{A}_{(jj'),(kk')}^{(\nu\mu)} \neq 0$, only if $|j - k| \le 1 \wedge |j' - k'| \le 1$ since $\operatorname{supp} N_j^2 \cap \operatorname{supp} N_k^2 = \emptyset$ for $|j - k| > 1$. Hence, $\mathbf{A}^{(\nu\mu)} \in \mathbb{R}^{d^2 \times d^2}$ in fact is sparse and block tridiagonal. The right-hand side $\mathbf{b} \in \mathbb{R}^{2d^2}$ is given accordingly as

$$\mathbf{b}_{(jj')}^{(\nu)} = -\int_0^T \int_\Omega \langle \phi_{j,j'}^{(\nu),2}(x_1, x_2), \nabla f(x_1, x_2, t)\rangle \, f_t(x_1, x_2, t)\, \mathrm{d}x\, \mathrm{d}t \,, \tag{23}$$

where $\nu = 1, 2$ and $1 \le j, j' \le d$. Having the solution β^* of $\mathbf{A}\beta^* = \mathbf{b}$ at hand we may compute

$$(\mathbf{u}_{d,2}^*)_\nu(x_1, x_2) = \sum_{j,j'=1}^{d} \beta_{jj'}^{*,\nu} N_j^2(x_1)\, N_{j'}^2(x_2) \,, \qquad \nu = 1, 2 \,. \tag{24}$$

Since the piecewise linear B-splines N_j^2 have the interpolation property, i.e. $N_j^2(x_1^{(k)}) = \delta_{jk}$, where δ_{jk} denotes the Kronecker symbol, we deduce from (24) that

$$(\mathbf{u}_{d,2}^*)_\nu(x_1^{(j)}, x_2^{(j')}) = \beta_{jj'}^{*,\nu} \,,$$

which simplifies the visualization of $\mathbf{u}^*_{d,2}$ at the pixels $\{(x_1^{(j)}, x_2^{(j')})\}$.
In our numerical experiments we compute the matrix entries $\mathbf{A}^{(\nu\mu)}_{(jj'),(kk')}$ as well as the right-hand side $\mathbf{b}^{(\nu)}_{(jj')}$ using the trapezoidal sum with step size $1/(2d)$ in x_1 and x_2 and $\delta t = T/N$ in the time variable t, where N denotes the number of image frames in the sequence f. The step size $1/(2d)$ was chosen to preserve the block tridiagonal structure of $\mathbf{A}^{(\nu\mu)}$. The derivatives f_{x_ν}, f_t were computed using the central differential quotient of order 2. Finally the arising system of linear equations $\mathbf{A}\beta^* = \mathbf{b}$ was solved applying a preconditioned CG-method where we used the Jacobian preconditioner. All sequences f consist of $N = 20$ frames of images with 64×64 pixels, that means $d = 64$. We assumed $T = 1$, what means that we normalized the frame distance in time to 1. Figures 2–4 show the first image of the sequence $f(x_1^{(j)}, x_2^{(j')}, 0)$ as well as the field $\mathbf{u}^*_{d,2}$ calculated as in (24). The image sequence in figure 2 consists of a Gaussian function moving from the upper left corner towards the center of the image. The sphere sequence illuminates a rotating sphere with bright spots. The taxi sequence finally consists of a taxi driving a right turn. The motion field is clearly visible in all these experiments. In 3 some regions seem to be stationary though there is a motion. The reason is, that in these regions the brightness does not change over time. A higher order spline or another function for Ψ might help. The optical flow in the lower left corner of figure 4 comes from the fact that there is another car entering the picture from the left. Figure 5 furthermore shows the optical flow between two subsequent frames only. Especially the optical flow of the taxi sequence is contaminated by noise. To denoise the input data we apply a pre-smoothing step to the image sequence $f(x_1, x_2, t)$ with a Gaussian filter

$$\begin{aligned} f_{\sigma,\tau}(x,t) &= \frac{\sigma^{-2}\tau^{-1}}{(2\pi)^{3/2}} \int_0^T \int_\Omega \mathrm{e}^{-\frac{\|x'-x\|^2}{2\sigma^2}}\, \mathrm{e}^{-\frac{|t'-t|^2}{2\tau^2}}\, f(x',t')\,\mathrm{d}x\,\mathrm{d}t\,, \\ & x = (x_1, x_2)\,, \qquad x' = (x_1', x_2')\,, \end{aligned} \tag{25}$$

where we chose $\sigma = 1/d$, $\tau = 2\delta t$. Figure 6 shows that the pre-smoothing in fact leads to a better result. The bright spots of the moving sphere are clearly visible as well as the flow field resulting from the car entering from the left in the taxi sequence.

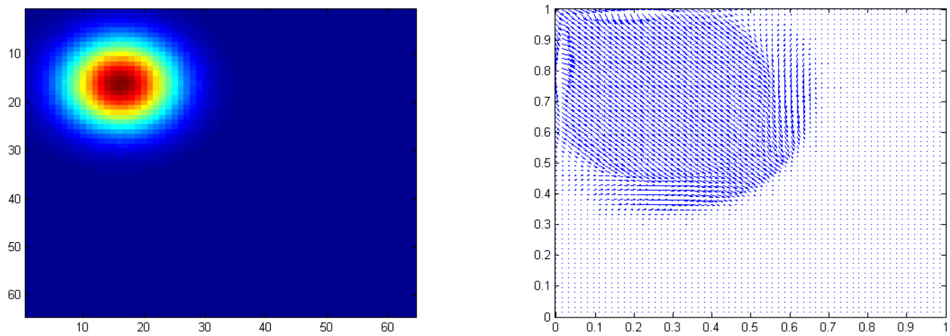

Figure 2: The left image shows the first frame of a test sequence consisting of a Gaussian function which moves from the upper left corner towards the image center. The optical flow field which emphasizes exactly this motion is displayed in the right image.

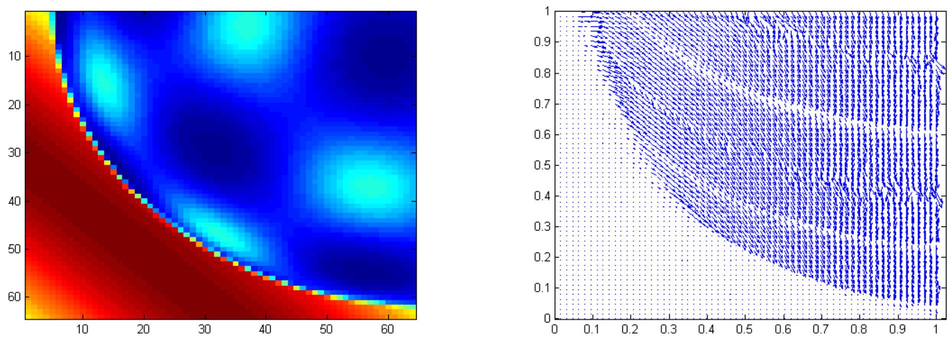

Figure 3: The left image shows the first frame of a test sequence consisting of a rotating sphere. The optical flow field is displayed in the right image. They are some stripes visible, where does not seem to be any motion though there is one.

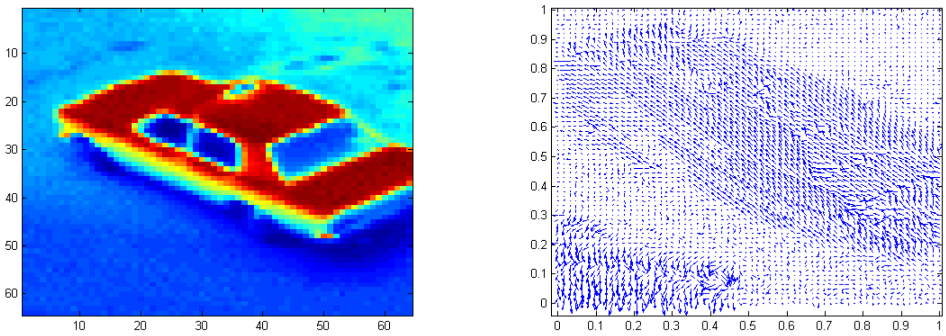

Figure 4: The left image shows the first frame of a test sequence consisting of a taxi making a right turn. From the left another car is entering the image frame. The optical flow field can be seen in the right image. Both motions are clearly visible.

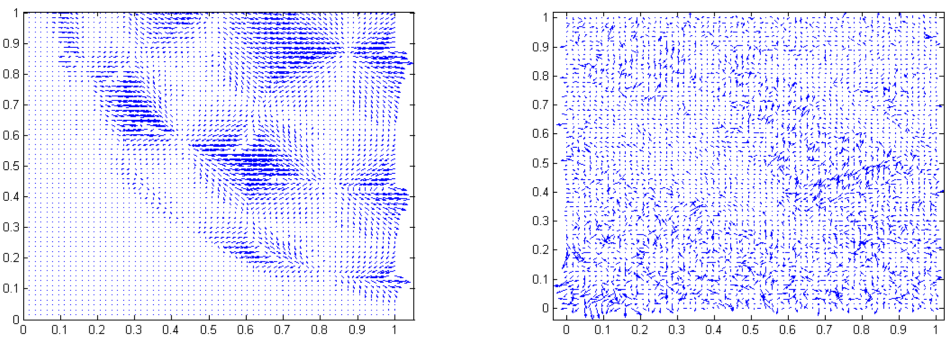

Figure 5: Optical flow between the frames 10 and 11 of the sphere sequence (left) and the taxi sequence (right) without a pre-smoothing step.

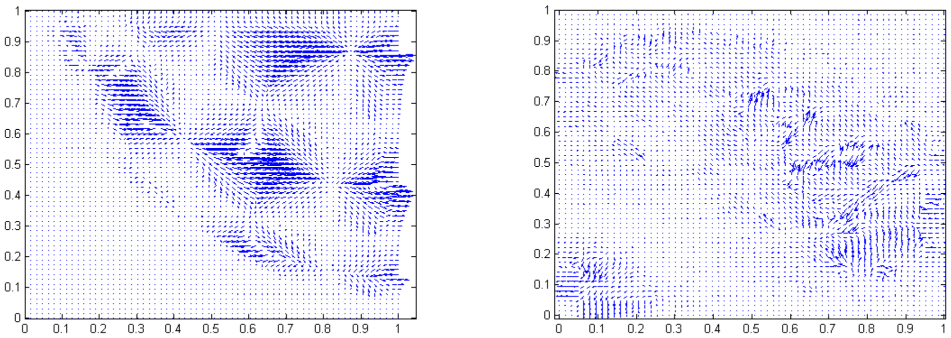

Figure 6: Optical flow between the frames 10 and 11 of the sphere sequence (left) and the taxi sequence (right) with the pre-smoothing (25) as denoising.

5.2 The gradient constancy assumption

Now we assume the gradient of brightness to be constant. That means we minimize E_Ψ as in (9) with

$$\mathbf{J}_f = \sum_{i=1}^{2} (\nabla f_{x_i} \otimes \nabla f_{x_i})$$

Using again the pieciewise linear tensor product B-splines (21) as basis functions we have to solve the system $\mathbf{A}\beta^* = \mathbf{b}$, where

$$\begin{aligned} \mathbf{A}^{(\nu\mu)}_{(jj'),(kk')} &= \int_0^T \int_\Omega \langle \phi^{(\nu),2}_{j,j'}, \mathbf{J}_f \phi^{(\mu),2}_{k,k'} \rangle \,\mathrm{d}x\,\mathrm{d}t \\ &= \int_0^T \int_\Omega [\mathbf{J}_f(x_1,x_2,t)]_{\nu\mu}\, N^2_j(x_1)\, N^2_{j'}(x_2)\, N^2_k(x_1)\, N^2_{k'}(x_2)\,\mathrm{d}x\,\mathrm{d}t \end{aligned}$$

for $1 \le \nu, \mu \le 2$, $1 \le j, j', k, k' \le d$, compare subsection 3.3. Again $\mathbf{A}^{(\nu\mu)} \in \mathbb{R}^{d^2 \times d^2}$ is sparse and block tridiagonal. The right hand side reads as

$$\mathbf{b}^{(\nu)}_{(jj')} = -\int_0^T \int_\Omega [\mathbf{J}_f(x_1,x_2,t)]_{3\nu}\, N^2_j(x_1)\, N^2_{j'}(x_2)\,\mathrm{d}x\,\mathrm{d}t\,,$$

where $\nu = 1, 2$ and $1 \le j, j' \le d$. We solve $\mathbf{A}\beta^* = \mathbf{b}$. Figure 7 shows the optical flow between the frames 10 and 11 of the sphere sequence, figure 8 that

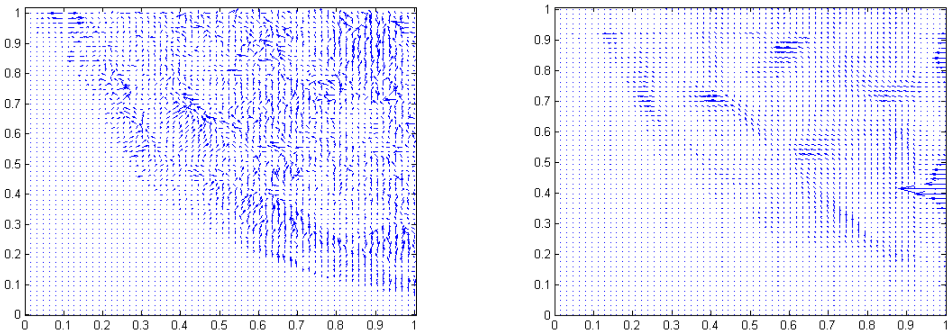

Figure 7: Optical flow between the frames 10 and 11 of the sphere sequence using the gradient of brightness constancy assumption. LEFT: Without smoothing. RIGHT: Including smoothing (25).

of the taxi sequence where the gradient of brightness constancy assumption was applied. We compared the results with and without the smoothing of the image data according to (25). Figure 9 displays the optical flows averaged over time of the sphere and the taxi sequence of figures 3, 4 but now with the gradient of brightness constancy assumption as structure tensor.

6 Conclusions

This article shows how optical flow can be calculated using a variational approach together with projection methods. If $\Psi(t) = t$, these projection methods always have optimal convergence rates in the sense that the residual error is of the same order as the approximation power of the applied basis functions. The method is easy to implement and first numerical results illustrate the feasability of the concept. In view of the error estimate (17) improvements can be expected when applying higher order B-splines, e.g. cubic splines ($m = 4$), or images with higher resolution (larger d). An additional pre-smoothing step of f can also lead to better reconstruction results. In order to make the basic ideas behind projections methods for optic flow estimation as transparent as possible, we have focused on a proof-of-concept that keeps the model assumptions relatively simple and allows a detailed mathematical analysis of the convergence rates. However, it is clear that projection approaches allow to integrate also more sophisticated models. Performing more research in this direction appears to be promising as future work. Particularly, if special properties of the optical flow field are desirable, e.g. a certain regularity or the incorporation of additional constaints, projec-

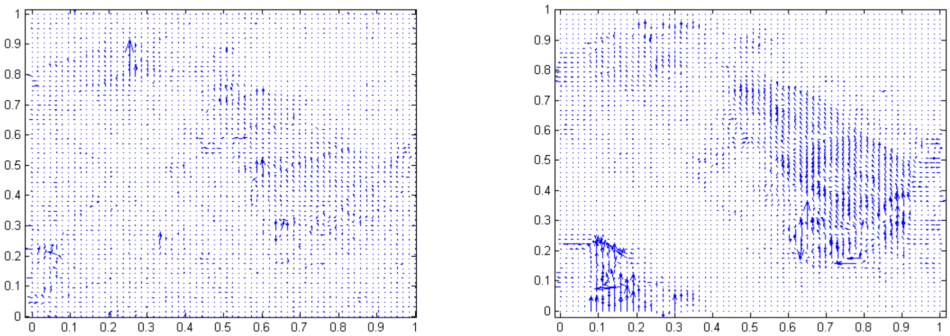

Figure 8: Optical flow between the frames 10 and 11 of the taxi sequence using the gradient of brightness constancy assumption. LEFT: Without smoothing. RIGHT: Including smoothing (25).

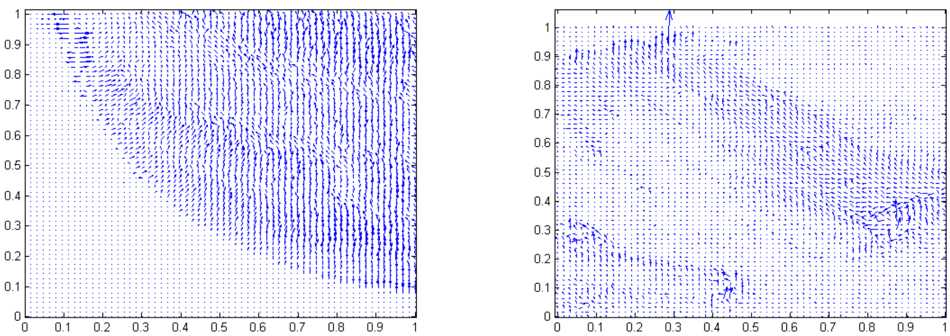

Figure 9: Optical flow of the sphere (picture to the left) and taxi sequence (picture to the right) with (10) as structure tensor.

tion methods can be an adequate and mathematically elegant tool to achieve them.

Acknowledgments

We thank Andrés Bruhn and Stephan Zimmer for helping us with data conversions. The taxi sequence has been taken from the web site

`http://i21www.ira.uka.de/image_sequences/`,

and the sphere sequence has been downloaded from

`http://www.katipo.otago.ac.nz/research/vision/`.

References

[1] L. Alvarez, J. Esclarín, M. Lefébure, and J. Sánchez, *A PDE model for computing the optical flow*, in Proc. XVI Congreso de Ecuaciones Diferenciales y Aplicaciones, Las Palmas de Gran Canaria, Spain, Sept. 1999, pp. 1349–1356.

[2] L. Alvarez, J. Weickert, and J. Sánchez, *Reliable estimation of dense optical flow fields with large displacements*, International Journal of Computer Vision, 39 (2000), pp. 41–56.

[3] T. Amiaz and N. Kiryati, *Dense discontinuous optical flow via contour-based segmentation*, International Journal of Computer Vision, 68 (2006), pp. 111–124.

[4] G. Aubert, R. Deriche, and P. Kornprobst, *Computing optical flow via variational techniques*, SIAM Journal on Applied Mathematics, 60 (1999), pp. 156–182.

[5] A. Bab-Hadiashar and D. Suter, *Robust optic flow computation*, International Journal of Computer Vision, 29 (1998), pp. 59–77.

[6] J. Barron, D. Fleet, and S. Beauchemin, *Performance of optical flow techniques*, International Journal of Computer Vision, 12 (1994), pp. 43–77.

[7] M. Bertero, T. A. Poggio, and V. Torre, *Ill-posed problems in early vision*, Proceedings of the IEEE, 76 (1988), pp. 869–889.

[8] M. J. Black and P. Anandan, *Robust dynamic motion estimation over time*, in Proc. 1991 IEEE Computer Society Conference on Computer Vision and Pattern Recognition, Maui, HI, June 1991, IEEE Computer Society Press, pp. 292–302.

[9] A. Borzi, K. Ito, and K. Kunisch, *Optimal control formulation for determining optical flow*, SIAM Journal on Scientific Computing, 24 (2002), pp. 818–847.

[10] T. Brox, A. Bruhn, N. Papenberg, and J. Weickert, *High accuracy optical flow estimation based on a theory for warping*, in Computer Vision – ECCV 2004, Part IV, T. Pajdla and J. Matas, eds., vol. 3024 of Lecture Notes in Computer Science, Springer, Berlin, 2004, pp. 25–36.

[11] T. Brox, A. Bruhn, and J. Weickert, *Variational motion segmentation with level sets*, in Computer Vision – ECCV 2006, Part I, H. Bischof, A. Leonardis, and A. Pinz, eds., vol. 3951 of Lecture Notes in Computer Science, Springer, Berlin, 2006, pp. 471–483.

[12] A. Bruhn and J. Weickert, *Towards ultimate motion estimation: Combining highest accuracy with real-time performance*, in Proc. Tenth International Conference on Computer Vision, vol. 1, Beijing, China, Oct. 2005, IEEE Computer Society Press, pp. 749–755.

[13] A. Bruhn, J. Weickert, T. Kohlberger, and C. Schnörr, *A multigrid platform for real-time motion computation with discontinuity-preserving variational methods*, International Journal of Computer Vision, 70 (2006), pp. 257–277.

[14] A. Bruhn, J. Weickert, and C. Schnörr, *Lucas/Kanade meets Horn/Schunck: Combining local and global optic flow methods*, International Journal of Computer Vision, 61 (2005), pp. 211–231.

[15] I. Cohen, *Nonlinear variational method for optical flow computation*, in Proc. Eighth Scandinavian Conference on Image Analysis, vol. 1, Tromsø, Norway, May 1993, pp. 523–530.

[16] B. Galvin, B. McCane, K. Novins, D. Mason, and S. Mills, *Recovering motion fields: an analysis of eight optical flow algorithms*, in Proc. 1998 British Machine Vision Conference, Southampton, England, Sept. 1998.

[17] S. Ghosal and P. Č. Vaněk, *Scalable algorithm for discontinuous optical flow estimation*, IEEE Transactions on Pattern Analysis and Machine Intelligence, 18 (1996), pp. 181–194.

[18] F. Glazer, *Multilevel relaxation in low-level computer vision*, in Multiresolution Image Processing and Analysis, A. Rosenfeld, ed., Springer, Berlin, 1984, pp. 312–330.

[19] W. Hinterberger, O. Scherzer, C. Schnörr, and J. Weickert, *Analysis of optical flow models in the framework of calculus of variations*, Numerical Functional Analysis and Optimization, 23 (2002), pp. 69–89.

[20] B. Horn and B. Schunck, *Determining optical flow*, Artificial Intelligence, 17 (1981), pp. 185–203.

[21] P. J. Huber, *Robust Statistics*, Wiley, New York, 1981.

[22] A. Kumar, A. R. Tannenbaum, and G. J. Balas, *Optic flow: a curve evolution approach*, IEEE Transactions on Image Processing, 5 (1996), pp. 598–610.

[23] A. Louis, *Inverse und schlecht gestellte Probleme*, Teubner, Stuttgart, 1989.

[24] B. Lucas and T. Kanade, *An iterative image reconstruction technique with an application to stereo vision*, in Seventh International Joint Conference on Artificial Intelligence, Vancouver, Canada, 1981, pp. 674–679.

[25] V. Maz'ja, *Sobolev Spaces*, Springer, Heidelberg, 1985.

[26] E. Mémin and P. Pérez, *Dense estimation and object-based segmentation of the optical flow with robust techniques*, IEEE Transactions in Image Processing, 7 (1998), pp. 703–719.

[27] ——, *Hierarchical estimation and segmentation of dense motion fields*, International Journal of Computer Vision, 46 (2002), pp. 129–155.

[28] A. Mitiche and P. Bouthemy, *Computation and analysis of image motion: a synopsis of current problems and methods*, International Journal of Computer Vision, 19 (1996), pp. 29–55.

[29] H.-H. Nagel, *Extending the 'oriented smoothness constraint' into the temporal domain and the estimation of derivatives of optical flow*, in Computer Vision – ECCV '90, O. Faugeras, ed., vol. 427 of Lecture Notes in Computer Science, Springer, Berlin, 1990, pp. 139–148.

[30] H.-H. Nagel and W. Enkelmann, *An investigation of smoothness constraints for the estimation of displacement vector fields from image sequences*, IEEE Transactions on Pattern Analysis and Machine Intelligence, 8 (1986), pp. 565–593.

[31] F. Natterer, *Regularisierung schlecht gestellter Probleme durch Projektionsverfahren*, Numerische Mathematik, 28 (1977), pp. 329–341.

[32] P. Nesi, *Variational approach to optical flow estimation managing discontinuities*, Image and Vision Computing, 11 (1993), pp. 419–439.

[33] N. Papenberg, A. Bruhn, T. Brox, S. Didas, and J. Weickert, *Highly accurate optic flow computation with theoretically justified warping*, International Journal of Computer Vision, 67 (2006), pp. 141–158.

[34] A. Rieder and T. Schuster, *The approximate inverse in action III: 3D-Doppler tomography*, Numerische Mathematik, 97 (2004), pp. 353–378.

[35] Y. Saad, *Iterative Methods for Sparse Linear Systems*, SIAM, Philadelphia, second ed., 2003.

[36] C. Schnörr, *Segmentation of visual motion by minimizing convex non-quadratic functionals*, in Proc. Twelfth International Conference on Pattern Recognition, vol. A, Jerusalem, Israel, Oct. 1994, IEEE Computer Society Press, pp. 661–663.

[37] L. Schumaker, *Spline Functions: Basic Theory*, Wiley, Chichester, 1981.

[38] C. Stiller and J. Konrad, *Estimating motion in image sequences*, IEEE Signal Processing Magazine, 16 (1999), pp. 70–91.

[39] R. Szeliski and J. Coughlan, *Spline-based image registration*, International Journal of Computer Vision, 22 (1997), pp. 199–218.

[40] S. Uras, F. Girosi, A. Verri, and V. Torre, *A computational approach to motion perception*, Biological Cybernetics, 60 (1988), pp. 79–87.

[41] J. Weickert, A. Bruhn, T. Brox, and N. Papenberg, *A survey on variational optic flow methods for small displacements*, in Mathematical Models for Registration and Applications to Medical Imaging, O. Scherzer, ed., Springer, Berlin, 2006, pp. 103–136.

[42] J. Weickert and C. Schnörr, *A theoretical framework for convex regularizers in PDE-based computation of image motion*, International Journal of Computer Vision, 45 (2001), pp. 245–264.

[43] G. Zini, A. Sarti, and C. Lamberti, *Application of continuum theory and multi-grid methods to motion evaluation from 3D echocardiography*, IEEE Transactions on Ultrasonics, Ferroelectrics, and Frequency Control, 44 (1997), pp. 297–308.